Acta Cryst. (1976). A32, 863

A Simple Model for Dynamical Neutron Diffraction by Deformed Crystals

BY G. ALBERTINI
Facoltà di Medicina, Università di Ancona, Italy

A. BOEUF
J.R.C. Euratom, Ispra, Italy, and Institut Laue–Langevin, 156X Centre de Tri, 38042 Grenoble Cedex, France

G. CESINI AND S. MAZKEDIAN
Facoltà di Ingegneria, Università di Ancona, Italy

S. MELONE
Facoltà di Medicina, Università di Ancona, Italy

AND F. RUSTICHELLI
Facoltà di Ingegneria, Università di Ancona, Italy; J.R.C. Euratom, Ispra, Italy; and Institut Laue–Langevin, 156X Centre de Tri, 38042 Grenoble Cedex, France

(*Received* 16 *February* 1976; *accepted* 19 *March* 1976)

A simple physical model is presented to predict the neutron diffraction properties of deformed crystals. The main interest of this model is its general applicability to deformed crystals and its mathematical simplicity. At first this model was applied to curved crystals and its validity was checked by comparison with the diffraction patterns obtained from the exact solution of the dynamical neutron diffraction theory. A comparison between the prediction of the model and experimental data in curved Si crystals is presented. Finally the model is used to predict neutron diffraction patterns by crystals with a gradient in the lattice spacing and by deformed crystals in the general case.

1. Introduction

The most recent contribution to the theoretical problem of X-ray diffraction by regularly deformed crystals has been presented by Katagawa & Kato (1974), who gave the exact wave fields for a spherical incident wave in the Laue case for a crystal having a constant strain gradient. Their work is based on the wave-optical theories developed by Takagi (1962, 1969) and Taupin (1964). Actually they were able to obtain exact analytical solutions of the Takagi–Taupin differential equations. These solutions are essentially expressed in terms of confluent hypergeometric functions.

Concerning the neutrons, some diffraction patterns by ideally curved crystals were calculated by Klar & Rustichelli (1973) by extending Taupin's dynamical theory. The results of the neutron diffraction calculations are substantially different from those relative to X-rays as a consequence of the low neutron absorption cross section. The neutron diffraction patterns were obtained by numerical solution of a complex differential equation.

Several neutron diffraction experiments were carried out on crystals with a gradient in the lattice spacing obtained by thermal gradient (Alefeld, 1969), on curved Ge crystals (Egert & Dachs, 1970), on Si crystals curved by chemical treatment (Antonini, Corchia, Nicotera & Rustichelli, 1972; Boeuf & Rustichelli, 1974), on thermally bent CaF_2 crystals (Kalus, Gobert & Schedler, 1973), on elastically curved Ge crystals (Kalus, 1975) and on elastically curved Si crystals (Frey, 1975). With the exception of Boeuf & Rustichelli (1974), none of the experimentalists has made a comparison of the data with the exact dynamical theories of diffraction by regularly distorted crystals.

In this paper we present a simple physical model for the deformed crystals, which allows the derivation of simple analytical expressions for the diffraction patterns by curved crystals, crystals with a gradient in the lattice spacing, and crystals of any kind of irregular deformation, in the Bragg case. The model is analogous to one used to evaluate the light diffraction properties of cholesteric liquid crystals with a pitch gradient (Mazkedian, Melone & Rustichelli, 1975) and offers a simple pictorial view of the physical phenomenon.

At first, the validity of the model will be checked by comparison with the neutron diffraction patterns obtained theoretically by Klar & Rustichelli (1973). Then the model will be used to interpret exhaustively the experimental results of Boeuf & Rustichelli (1974). Finally the use of the model in the prediction of diffraction patterns by crystals with a gradient in the lattice spacing and by crystals with any kind of irregular distortion, will be discussed.

2. Description of the model for curved crystals

Neutron diffraction by a curved non-absorbing crystal in the Bragg law will be considered. The curved crystal will be divided into three regions, by analogy with the model of a cholesteric liquid crystal with a pitch gradient (Mazkedian, Melone & Rustichelli, 1975). The

notation of Klar & Rustichelli (1973) will be used: c is a quantity associated with the crystal curvature, A the distance of a given lattice plane from the surface of the crystal, y the deviation from the Bragg law of this plane, $y(0)$ the deviation from the Bragg law at the surface of the crystal. In these units (see also Zachariasen, 1967) the extinction length corresponds to $A=2$ and the halfwidth ($w_D/2$) of the Darwin curve is equal to $y=1$; c is defined in Klar & Rustichelli (1973) by

$$c=\frac{\mathrm{d}y}{\mathrm{d}A}. \tag{1}$$

In these units $c=1$ corresponds to the optimal curvature. From (1) is easily derived (29) of Klar & Rustichelli (1973)

$$y=y(0)+cA. \tag{2}$$

Let us suppose that the crystal is oriented with respect to a monochromatic impinging neutron beam of wavelength λ in such a way that there exists a plane at the depth A_B inside the crystal for which the Bragg law is exactly verified, *i.e.* y is equal to zero. Then from (2) one obtains

$$A_B=\frac{y(0)}{c}. \tag{3}$$

A_B will constitute the depth of the plane located at the centre of region II. The upper limit ${}_uA_{II}$ and the lower limit ${}_lA_{II}$ of region II (Fig. 1) are defined by

$$\begin{aligned} y({}_uA_{II})&=-1\\ y({}_lA_{II})&=+1. \end{aligned} \tag{4}$$

Condition (4) becomes, by use of (2):

$$\begin{aligned} {}_uA_{II}&=-\frac{[1+y(0)]}{c}\\ {}_lA_{II}&=\frac{1-y(0)}{c}. \end{aligned} \tag{5}$$

As the condition $-1<y<1$ defines the total reflexion range of the Darwin curve (Zachariasen, 1967) region II corresponds to the volume of the curved crystal for which the deviation from the Bragg law is contained inside the total reflexion range. This allows us to assume, in analogy with the model of Mazkedian, Melone & Rustichelli (1975), that region II diffracts neutrons as a perfect crystal of the same thickness and having the orientation as the middle plane A_B, *i.e.* $y=0$.

The reflectivity of a perfect non-absorbing crystal is (Zachariasen, 1967) for X-rays

$$r=\frac{\sin^2(A\sqrt{y^2-1})}{y^2-1+\sin^2(A\sqrt{y^2-1})}. \tag{6}$$

(6) can also be used to evaluate reflectivity in the case of neutron diffraction if the proper neutron quantities are inserted in the definitions of A and y (Klar & Rustichelli, 1973). As a consequence, (6) can be used to evaluate the reflectivity r_{II} of region II from the total thickness A_{II} of region II which can be deduced from (5)

$$A_{II}=\frac{2}{c} \tag{7}$$

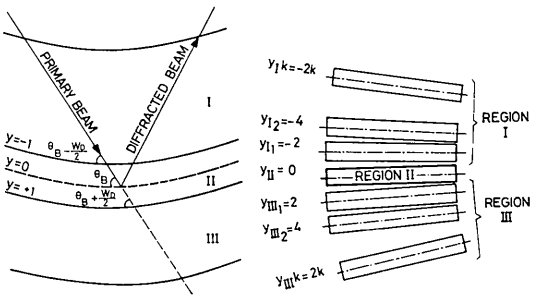

(*a*) (*b*)

Fig. 1. Schematic representation of the model for a curved crystal; (*a*) shows the different regions in the actual crystal and (*b*) shows how the model consisting of perfect crystals is built up.

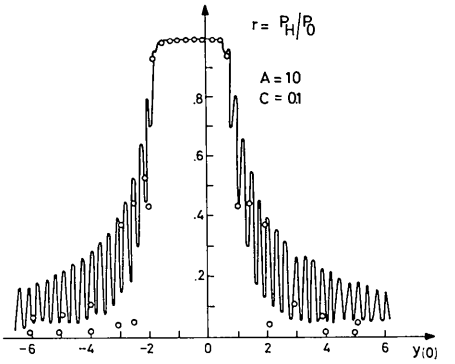

Fig. 2. Comparison of the model predictions with the exact dynamical theory for a curved crystal with a curvature $c=0{\cdot}1$ and a thickness $A=10$. The full line is the neutron diffraction pattern calculated by the exact dynamical theory (Klar & Rustichelli, 1973). The small circles are the values calculated by the model.

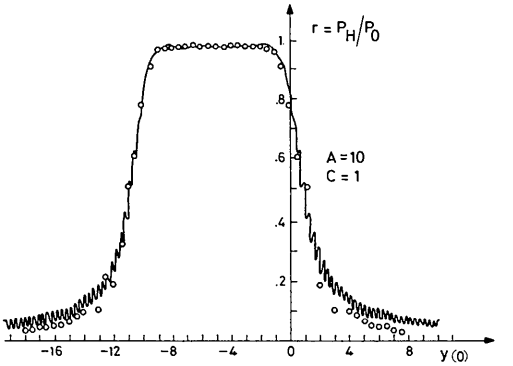

Fig. 3. Comparison of the model predictions with the exact dynamical theory for a curved crystal with a curvature $c=1$ and a thickness $A=10$. The full line is the neutron diffraction pattern calculated with the exact dynamical theory (Klar & Rustichelli, 1973). The small circles are the values calculated by the model.

and by insertion of the value $y=0$ which represents the average orientation of region II. The result is

$$r_{II}=\tanh^2\left(\frac{2}{c}\right)^2. \tag{8}$$

Once region II is defined, regions I and III are implicitly defined (Fig. 1). At this stage one could approximate regions I and III with perfect crystals of the same thickness (Mazkedian, Melone & Rustichelli, 1975). Then the reflectivity of the crystal would be given by

$$r=1-(1-r_I)(1-r_{II})(1-r_{III}). \tag{9}$$

However, to increase the accuracy of the model each of regions I and III will be subdivided into many perfect crystals having the same thickness as region II and as a consequence a misorientation $\Delta y=2$, each one with respect to the adjacent one. In such a way the middle planes of the many perfect crystals maintain the same orientation as in the actual curved crystal. By indexing the perfect crystals in regions I and III starting from the crystal adjacent to region II (Fig. 1), one can calculate the reflectivity r_{IK} (or r_{IIIK}) of the perfect crystal K of region I (or III) from (6) by inserting the values:

$$A_{IK}=\frac{2}{c}, \qquad A_{IIIK}=\frac{2}{c}$$
$$y_{IK}=-2K, \qquad y_{IIIK}=+2K. \tag{10}$$

The reflectivity r_I (or r_{III}) of region I (or III) can be derived by the same principle underlying (9) which leads to the expression

$$r_I=1-\prod_{k=1}^{n_I}(1-r_{IK}), \quad r_{III}=1-\prod_{k=1}^{n_{III}}(1-r_{IIIK}) \tag{11}$$

where n_I and n_{III} are the number of perfect crystals in which regions I and III are decomposed, respectively.

By inserting the obtained values for r_I, r_{II}, r_{III} in (9) one obtains the value for the reflectivity $r=P_H/P_0$ of the curved crystal, for a given orientation $y(0)$ of the crystal itself, with the neutron wavelength λ and the curvature c being imagined fixed and considered as parameters. By varying $y(0)$ one obtains the rocking curve $r=r[y(0)]$. It is clear physically that by changing $y(0)$ the location of region III changes, as can be seen from (3) and (5), and the quantities n_I and n_{III} also change. For certain values of $y(0)$ regions I or III, and eventually region II, can disappear.

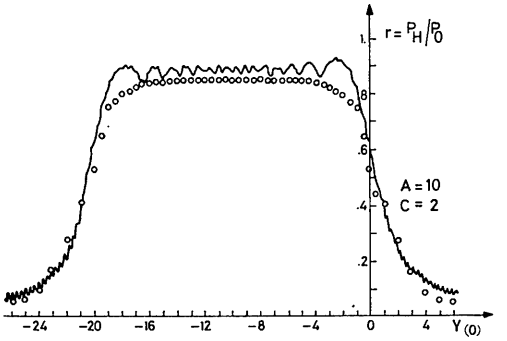

Fig. 4. Comparison of the model predictions with the exact dynamical theory for a curved crystal with a curvature $c=2$ and a thickness $A=10$. The full line is the neutron diffraction pattern calculated with the exact dynamical theory (Klar & Rustichelli, 1973). The small circles are the values calculated by the model.

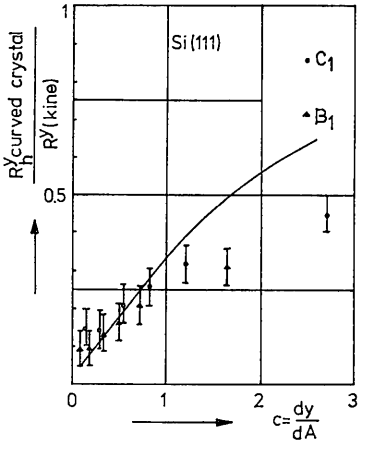

Fig. 5. Comparison between the curve deduced from the theoretical model and the experimental data (Boeuf & Rustichelli, 1974). The experimental points represent the integrated reflecting power normalized by the kinematical reflecting power as a function of the crystal curvature for the (111) plane and the 1 mm thick crystals. Points B_1 and C_1 correspond to an actual curvature of the crystal of 90 and 55 m respectively.

3. Application of the model to practical cases

3.1 *Comparison with the exact dynamical theory*

It is clear that the model is quite simplified and must be checked before being applied. Therefore the rocking curves $r=r[y(0)]$ obtained by the model were compared with those reported by Klar & Rustichelli (1973) which were deduced by applying the exact dynamical theory of neutron diffraction. The comparison was performed for a crystal of thickness $A=10$ (*i.e.* equal to five extinction lengths) and for three values of curvature ($c=0{\cdot}1, c=1, c=2$). The results of the comparison are shown in Figs. 2, 3 and 4 where the circles represent the r values obtained by the model. It appears that the agreement is quite satisfactory, with a slight discrepancy for the largest c value.

3.2 *Comparison with experimental data on curved silicon crystals*

The theoretical predictions of the model were compared with the experimental data obtained by Boeuf & Rustichelli (1974) on curved Si crystals. In this experiment the ratio between plane and curved Si crystals was measured as a function of the neutron wavelength with different reflecting planes. As a consequence of

theoretical considerations, the experimental data were rearranged in such a way that for each reflexion the ratio between the integral reflecting power (R_h^y) of the curved crystal and the corresponding kinematical reflecting power [R_h^y(kine)] could be plotted as a function of the curvature c. Fig. 5 shows the comparison between experiment and the theoretical curve deduced from the model for the (111) reflecting plane of 1 mm thick crystals. Fig. 6 shows the comparison for the (111) reflecting plane of 0·5 mm thick crystals. Figs. 7 and 8 show the comparison for the (551) reflecting plane of 1 mm and 0·5 mm thick crystals, respectively. Fig. 9 shows the comparison for the (115) reflecting plane of 1 mm thick crystals. The agreement is generally satisfactory, taking into account that neutron absorption is not included in the model, with the exception of the (115) plane. However the discrepancy in this case can be explained by the non-absolute perfection of the crystals used before curvature. In fact at so low a curvature the intrinsic imperfection of the crystal becomes more relevant than the curvature effect.

4. Neutron diffraction by crystals with a gradient in lattice spacing

The model developed in § 2 for curved crystals can be directly extended to predict neutron diffraction patterns from crystals with a gradient in the lattice spacing. In fact it will be shown that a crystal with a given gradient (grad d) in the lattice spacing d is equivalent, as far as the neutron diffraction properties are concerned, to a curved crystal having a certain curvature c, which is a function of grad d and of the crystallographic characteristics of the crystal. It will be supposed that the crystal has a pure lattice gradient without any curvature of the diffracting planes and that the gradient is perpendicular to the surface of the crystal (for the most general case see the Appendix). Then at a depth Δt below the surface of the crystal the variation Δd in the lattice spacing is

$$\Delta d(\Delta t)=(\text{grad } d)\Delta t\,. \tag{12}$$

This Δd will introduce a deviation from the Bragg law corresponding to a certain value $y(\Delta t)$ which could be imagined to be introduced also by a misorientation $\Delta\theta(\Delta t)$ due to a certain curvature c to be determined. In order to calculate c we use the differentiated Bragg equation

$$\frac{\Delta\lambda}{\lambda}=(\cot\theta)\Delta\theta+\frac{\Delta d}{d} \tag{13}$$

in which $\Delta\lambda/\lambda$ is assumed to be zero. By inserting the $\Delta d(\Delta t)$ and $\Delta\theta(\Delta t)$ in (13) one obtains

$$\Delta\theta(\Delta t)=-\frac{\text{grad } d}{d}(\tan\theta)\Delta t\,. \tag{14}$$

On the other hand in a crystal of curvature radius ϱ the angular misorientation along the incident beam at a depth Δt is given [see for instance equation (5) of Klar & Rustichelli, 1973] by

$$\Delta\theta(\Delta t)=\frac{\Delta t}{\varrho}\cot\alpha\,. \tag{15}$$

By equating (14) and (15) one obtains the value of ϱ equivalent to a given grad d. In order to express ϱ in units of c, defined above, one can use equation (10) of Boeuf & Rustichelli (1974)

$$\varrho=\frac{1}{c}\left(\frac{t_{\text{ext}}}{\Delta\theta(\text{Darwin})}\right)\cot\alpha\,. \tag{16}$$

From (14), (15) and (16), one obtains

$$c=\frac{\text{grad } d}{d}t_{\text{ext}}\left(\frac{\tan\theta}{\Delta\theta(\text{Darwin})}\right). \tag{17}$$

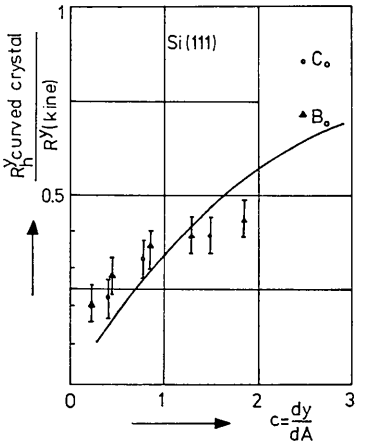

Fig. 6. Comparison between the curve deduced from the theoretical model and the experimental data (Boeuf & Rustichelli, 1974). The experimental points represent the integrated reflecting power normalized by the kinematical reflecting power as a function of the crystal curvature for the (111) plane and the 0·5 mm thick crystals. Points B_0 and C_0 correspond to an actual curvature of the crystal of 35 and 20 m respectively.

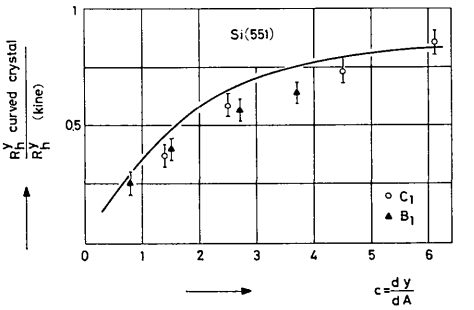

Fig. 7. Comparison between the curve deduced from the theoretical model and the experimental data (Boeuf & Rustichelli, 1974). The experimental points represent the integrated reflecting power normalized by the kinematical reflecting power as a function of the crystal curvature for the (551) plane and the 1 mm thick crystals. Points B_1 and C_1 correspond to an actual crystal curvature of 90 and 55 m respectively.

(17) states that a crystal with a given gradient will give rise to a diffraction pattern equal to a curved crystal with a curvature c given by (17) itself.

Table 1 lists the equivalence obtained by (17) between grad d and c for different reflexions of different crystals at the neutron wavelength $\lambda = 1{\cdot}2$ Å.

5. Conclusion

A simple model was used to predict, in an approximative way, neutron diffraction patterns by curved crystals, crystals with a gradient in the lattice spacing and deformed crystals in the general case. Some of these cases can be treated by rigorous and sophisticated theories, with which the present model does not pretend to compete. The interest of the model is its general applicability to deformed crystals and its extreme simplicity, being based only on the concept of width of the Darwin curve and of reflectivity by a perfect crystal of finite thickness. This makes it easily applicable by any experimentalist. The model was checked with the results of a rigorous application of the Taupin dynamical theory of diffraction by deformed crystals. Then it was applied to the interpretation of a recent neutron diffraction experiment on curved Si crystals.

Table 1. *Values of grad d for different reflexions of various crystals at the neutron wavelength* $\lambda = 1{\cdot}2$ Å

	Reflecting plane *hkl*	grad d corresponding to $c=1$	$1/d$ grad d corresponding to $c=1$ % cm^{-1}
Si	111	$2{\cdot}72\times10^{-10}$	0·867
	333	$1{\cdot}13\times10^{-11}$	0·299
	555	$9{\cdot}90\times10^{-12}$	0·158
Ge	111	$0{\cdot}97\times10^{-10}$	0·296
	333	$1{\cdot}04\times10^{-11}$	0·096
	555	$1{\cdot}04\times10^{-12}$	0·016
Al	111	$1{\cdot}61\times10^{-10}$	0·689
	222	$0{\cdot}81\times10^{-11}$	0·069
	333	$1{\cdot}17\times10^{-12}$	0·015
Be	100	$4{\cdot}18\times10^{-10}$	2·13
	200	$2{\cdot}25\times10^{-11}$	0·229
Cu	111	$2{\cdot}19\times10^{-10}$	1·05

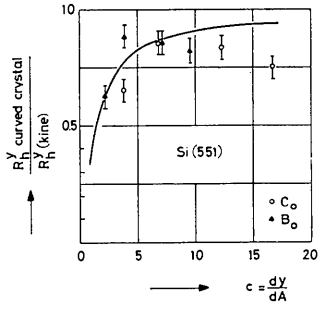

Fig. 8. Comparison between the curve deduced from the theoretical model and the experimental data (Boeuf & Rustichelli, 1974). The experimental points represent the integrated reflecting power normalized by the kinematical reflecting power as a function of the crystal curvature for the (551) plane and the 0·5 mm thick crystals. Points B_0 and C_0 correspond to an actual crystal curvature of 35 and 20 m respectively.

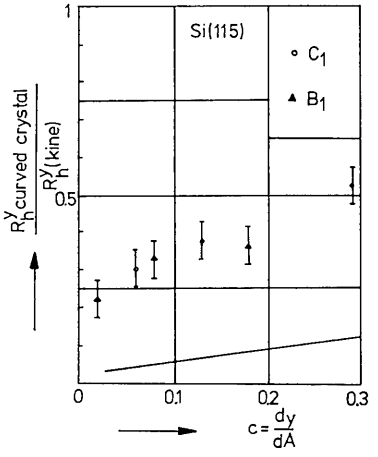

Fig. 9. Comparison between the curve deduced from the theoretical model and the experimental data (Boeuf & Rustichelli, 1974). The experimental points represent the integrated reflecting power normalized by the kinematical reflecting power as a function of the crystal curvature for the (115) plane and the 1 mm thick crystal. Points B_1 and C_1 correspond to an actual crystal curvature of 90 and 55 m respectively.

APPENDIX

Neutron diffraction by a deformed crystal in the general case

Let us consider a deformed crystal in which an arbitrary deformation exists as a function of depth A below the surface. The only restriction made on the character of the deformation is that for each value of A along the path of the primary neutron beam, the values of lattice plane orientation and lattice parameters can be defined. As a consequence the function $y(A)$ is defined for each value of A once the orientation of the crystal $y(0)$ is known. In order to obtain $y(A)$ one could use equations (18) and (25) of Klar & Rustichelli (1973). However it is perhaps easier to imagine that the misorientation of the lattice plane at depth A, as compared to the plane $A=0$, is due to an average curvature which can be easily calculated by geometrical considerations. This curvature can be expressed in units of c and allows the evaluated insertion in (7). As a consequence, this same equation permits the evaluation of $y_\theta(A)$ due to the plane misorientation. In an analogous way one can calculate from the result of § 4, the value of $y_d(A)$ due to the variation of the lattice spacing at depth A relative to that at $A=0$. The function $y(A)$ is obtained as a sum of $y_\theta(A)$ and $y_d(A)$. Once function $y(A)$ is obtained, the zero values $(A_{B1}, A_{B2}, \ldots, A_{Bn})$ will correspond to the lattice planes satisfying the Bragg equation. Fig. 10 represents a generic function $y(A)$ which, for the sake of simplicity, is supposed to be continuous, although the following considerations can also be applied in case of discontinuity.

With each zero value, *i.e.* to each A_{Bj}, will be associated a so-called region II, defined as in the case of curved crystals, by (4), namely by the condition $-1 \leq y \leq 1$. This definition is visualized in Fig. 10. Obviously the thickness of each region II will depend on the slope of the function $y(A)$ at the given A_{Bj}. It is supposed that the set of regions II can be treated as a unique perfect crystal whose reflectivity can be calculated by (8) where the A value is obtained by summation of all the region II thicknesses. Once set II is defined, the remaining deformed crystal will be subdivided into several sets, each one determined by the condition $\Delta y = 2$, starting from the boundary of set II. Thus a first set will be determined by the A value, satisfying the condition $+1 < y(A) < +3$, a second set by $+3 < y < +5$, and so on in analogy with the model presented in Fig. 1 for the case of a curved crystal. Each one of these sets, as for set II, will be supposed to consist of perfect regions having the same orientation of the middle plane. Each one of the sets in which the remaining part of the crystal is decomposed has a neutron reflectivity r_j given by (6). The thickness A will again be obtained by the summation of all the corresponding regions. In such a way the deformed crystal has been divided into a series of perfect crystal regions including set II, whose reflectivities can be calculated by (6) or (8). Then, by calling r_j the reflectivity of the generic perfect crystal set, the total reflectivity of the deformed crystal is given by

$$r_d = 1 - \prod_{j=1}^{n} (1 - r_j) \qquad (18)$$

in analogy with (9) or (11) where n is the number of sets obtained for a given crystal orientation.

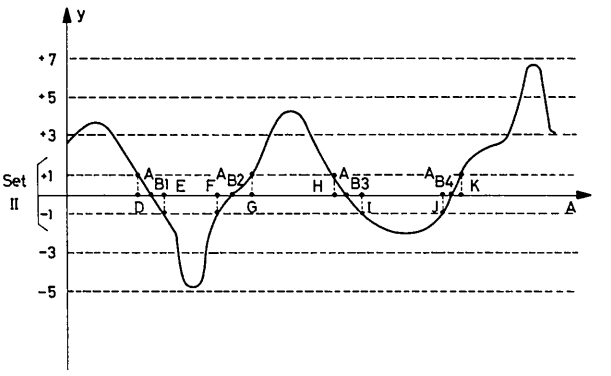

Fig. 10. $y(A)$ represents a generic deformation of a crystal as a function of thickness A. The zero values of functions A_{B1}, A_{B2}, A_{B3} and A_{B4} represent the depth of the crystal at which the Bragg law is satisfied. At each one of these zero points is associated a region II determined by the condition $-1 < y < +1$. The different regions II are given by the crystal parts with A values included between *DE*, *FG*, *HI* and *JK* respectively.

References

ALEFELD, B. (1969). *Z. Phys.* **228**, 454–464.

ANTONINI, M., CORCHIA, M., NICOTERA, E. & RUSTICHELLI, F. (1972). *Nucl. Instrum. Meth.* **104**, 147–152.

BOEUF, A. & RUSTICHELLI, F. (1974). *Acta Cryst.* A**30**, 798–805.

EGERT, G. & DACHS, H. (1970). *J. Appl. Cryst.* **3**, 214–220.

FREY, F. (1975). *Nucl. Instrum. Meth.* **125**, 9–17.

KALUS, J. (1975). *J. Appl. Cryst.* **8**, 361–364.

KALUS, J., GOBERT, G. & SCHEDLER, E. (1973). *J. Phys. E*, **6**, 488–492.

KATAGAWA, T. & KATO, N. (1974). *Acta Cryst.* A**30**, 830–836.

KLAR, B. & RUSTICHELLI, F. (1973). *Nuovo Cim.* **13***B*, 249–272.

MAZKEDIAN, S., MELONE, S. & RUSTICHELLI, F. (1975). *J. de Phys.* **36**, 283–287.

TAKAGI, S. (1962). *Acta Cryst.* **15**, 1311–1312.

TAKAGI, S. (1969). *J. Phys. Soc. Japan*, **26**, 1239–1253.

TAUPIN, D. (1964). *Bull. Soc. fr. Minér. Crist.* **87**, 469–511.

ZACHARIASEN, W. H. (1967). *Theory of X-ray Diffraction*, pp. 111–129. New York: Dover.